Validation and Application of a Mask Model for Inverse Lithography

Thuc H. Dam, Xin Zhou, Dongxue Chen, Anthony Adamov, Danping Peng, & Bob Gleason
Luminescent Technologies, 2471 East Bayshore Road Suite 600, Palo Alto, CA 94303

ABSTRACT

As photomask critical dimensions shrink significantly below the exposure wavelength and the angle of off-axis illumination increases, the use of Kirchhoff thin mask approximation cannot capture diffraction and polarization effects that occur at a topographical mask surface. Such approximation errors result in inaccurate models that lead to poor prediction for image simulation, which can waste time and money during lithographic process development cycle. The real effects of a thick mask can be simulated using finite difference time domain (FDTD) electromagnetic (EM) field calculations, or be better approximated with less error using such techniques such as boundary layer or various Fourier transformation techniques.

Keywords: inverse lithography, ILT, computational lithography, OPC, RET, lithography, DFM

1. INTRODUCTION

As the mask pitch becomes significantly less than the wavelength of a DUV system, and the angle of off-axis illumination becomes increasingly greater than normal incident beam, Kirchhoff thin mask approximation may provide a greater image intensity error relative to thick mask calculation, which can account for real physical/topographical effects on transmission and polarization of light as it travels through a mask. Such approximation errors result in inaccurate models that lead poor accuracy and prediction for wafer simulation. Although it is possible to simulate these real effects with rigorous EM calculations, the computational cost is too expensive to employ for full chip.

There are two published approaches to approximating 3D mask effects that can be computationally more efficient than FDTD. One method utilizes a locally applied spatial boundary regions at every Kirchhoff edge. The boundary width and transmission/polarization parameters can be varied or calibrated to project an aerial image that closely approximates an aerial image created by a rigorous EM calculation. Luminescent's spatial domain approach is a proprietary extension of the published Boundary Layer Model, which is suitable for source-mask-joint-optimization.**[1]** Another approach uses 2D Fourier transform in the frequency domain of the mask transmittance function. The transformed mask image representation can be filtered with various shapes and frequency to closely approximate an aerial image created by a rigorous EM calculation. Luminescent's frequency domain approach is a proprietary extension of the vector-formulated Hopkins equation, which is suitable for full-chip simulation with a fixed optics.**[2,3,4]**

Luminescent has parallel implementations for both of these approaches, and customers can decide on which of the two to use. Due to its suitability for full-chip simulation, this paper discusses the application and results for frequency domain approximation (FDA) within Luminescent's inversion process. First, FDA calibration process and specific results will be shared. In particular, results containing aerial image intensity profiles for various features simulated with FDA will be compared against images from Panoramic's rigorous FDTD 3D mask calculation and Kirchhoff approximation. Secondly, a calibrated FDA model will be applied to test targets during inversion (ILT) process. The resulting FDA ILT mask designs will be compared with respective Kirchhoff ILT mask designs. Panoramic simulation results (Kirchhoff-approximated and FDTD-calculated) of each respective mask will also be presented.

2. EXPERIMENTAL

2.1 FDA Calibration Process

The calibration process begins by generating a set of reference data by FDTD calculation in Panoramic's EM Suite. Luminescent's FDA model is generated by modifying TCC coefficients until calibration results match a set of FDTD data. During the calibration of the TCC coefficients, an algorithm minimizes RMS error between reference FDTD aerial image intensities and their corresponding FDA image intensities at every pixel within an intensity range. This minimization algorithm seeks a unique solution for the set of input reference data points. The reference data set contains aerial image intensity computed in the middle of 200nm thick resist for the following set of patterns, mask type and illumination setup:

- 48 line/space patterns with multiple SRAF insertions (single band)
  - Line width = 100 nm
  - SRAF CD = 25, 30, & 35 nm
  - Pitch = 250 – 600 nm in 50 nm increments
- 79 contact arrays
  - Contact CD = 80-100 nm in 5 nm increments
  - Pitch = 300 nm and 100-250 nm in 10 nm increments
- 6% EPSM mask
- Unpolarized 193 nm annular illumination σ_{in}/σ_{out} =0.95/0.65, NA=1.1

For each pattern permutation, for example 100 nm line in pitch 550 with 25 nm SRAF, the collected data contains intensity profiles with: 1) Luminescent's Kirchhoff approximation, 2) Luminescent's FDA and 3) Panoramic FDTD calculation. The differences between 1&2 and 2&3 are also compared.

2.2 Inversion with FDA

Given two targets, one containing an isolated square (100x100nm) and another containing 1xN array of rectangles (80x400 nm in 350 nm pitch) [Fig. 1], an inversion recipe was created with the following setup parameters:

- MRC = 20 nm
- EPE = 5% CD
- 6% EPSM mask
- X/Y Polarized 193 nm 35° dipole illumination σ_{in}/σ_{out} =0.97/0.82, NA=1.2 [Fig. 1c]
- Image and focus plane on top of 200nm thick resist with standing wave averaging enabled.
- Kirchhoff approximated constant threshold resist (CTR) model with 0.1 threshold

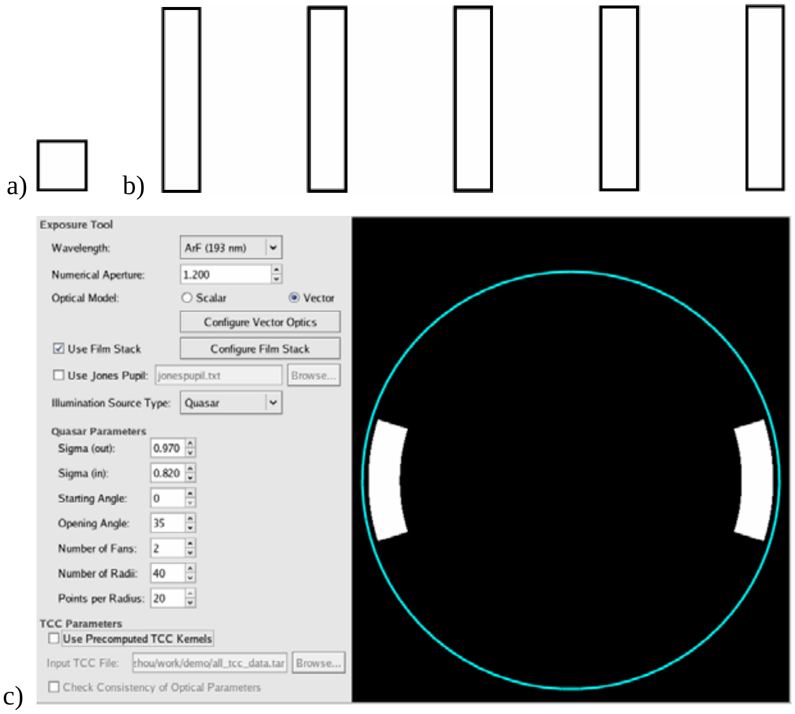

Exposure Tool
Wavelength: ArF (193 nm)
Numerical Aperture: 1.200
Optical Model: ○ Scalar ● Vector
Configure Vector Optics
☑ Use Film Stack
Configure Film Stack
☐ Use Jones Pupil: jonespupil.txt
Browse...
Illumination Source Type: Quasar
Quasar Parameters
Sigma (out): 0.970
Sigma (in): 0.820
Starting Angle: 0
Opening Angle: 35
Number of Fans: 2
Number of Radii: 40
Points per Radius: 20
TCC Parameters
☐ Use Precomputed TCC Kernels
Input TCC File: :hou/work/demo/all_tcc_data.tar
Browse...
☐ Check Consistency of Optical Parameters

Figure 1. a) 100x100 nm isolated square target. b) 1xN array of rectangles (80x400 nm in 350 nm pitch). c) Illumination setup for simulation and inversion.

An FDA model calibration was conducted with a subset of patterns from 2.1 with a dipole illumination setup as described in the 2.2 Kirchhoff setup. For comparison, FDA and Kirchhoff models were separately applied during each pattern's inversion. The resulting FDA and Kirchhoff ILT solutions were then simulated with FDTD calculation and Kirchhoff approximation with the above illumination configurations. The intensity profiles of this matrix was collected and compared: 1) FDA ILT simulated with Kirchhoff, 2) FDA ILT simulated with FDTD, 3) Kirchhoff ILT simulated with Kirchhoff, and 4) Kirchhoff ILT simulated with FDTD.

3. RESULTS AND DISCUSSIONS

3.1 FDA Calibration Results and Discussions

Prior to calibration, a set of nested line calibration structures described in 2.1 were simulated with Kirchhoff approximation in Luminescent's software. The intensity profiles from these images were directly compared to their respective FDTD simulation profiles. In figure 2a, one set of these profiles was compared for a 100 nm line in 550 nm pitch with three 25 nm SRAF. It showed that the FDTD intensity was relatively lower than Luminescent's Kirchhoff simulation results. Once a Luminescent's calibrated FDA model was applied, the intensity difference became significantly lowered (Figure 2b). The differences between Luminescent's simulation and FDTD calculations for the entire calibration set were plotted in Figure 3. The general trends indicated that Kirchhoff approximation differences increase with increasing pitch (more open space) for the nested line structures. The larger intensity differences between FDTD and Luminescent's Kirchhoff at higher pitches were contributed by the small SRAF's placed in between the main features. Luminescent's implementation of a calibrated FDA model generally reduced relative intensity differences significantly.

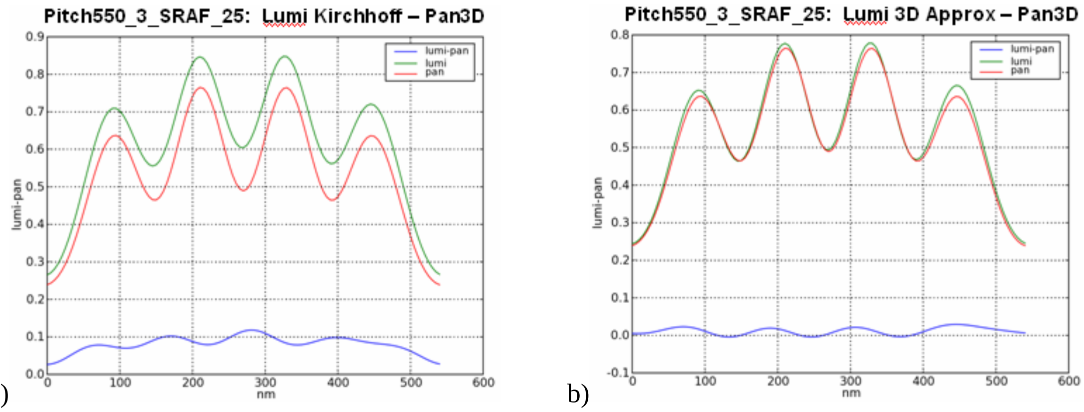

a) b)

Figure2. 100 nm line in 550 nm pitch with 3 SRAFs simulated with a) Luminescent's Kirchhoff approximation and b) Luminescent's 3D calibrated model. Luminescent's 3D approximation closely matches that of Panoramic's FDTD calculations.

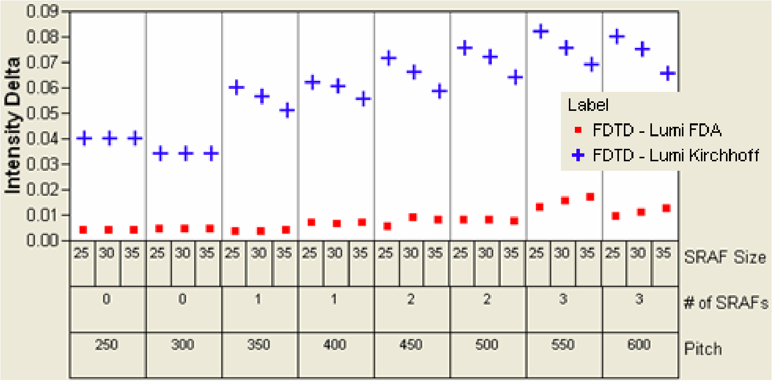

Figure 3. Graph shows the intensity error differences for nested line space patterns between Luminescent's Kirchhoff and 3D approximation relative to FDTD.

Similar simulation studies were conducted on a set of calibration contacts as described in section 2.1. Contacts simulated with Luminescent's Kirchhoff approximation showed higher intensity delta relative to FDTD calculated intensity, while those simulated with Luminescent's calibrated FDA had significantly lower intensity delta. Figure 4 displayed one such example for a 100 nm contact in 120 nm pitch. With small delta in intensity between FDA and FDTD, a grid difference between Luminescent's FDA simulation and Panoramic FDTD simulation caused the apparent asymmetric intensity delta in Figure 4b. Figure 5 showed a plot containing the intensity differences for contacts in the calibration set. This data indicated that Kirchhoff approximation for contacts in relatively tighter pitches could have higher intensity profile differences compared to FDTD calculations. As with the line space calibration set, Luminescent's implementation of a calibrated FDA model for contacts also generally reduced relative intensity differences significantly.

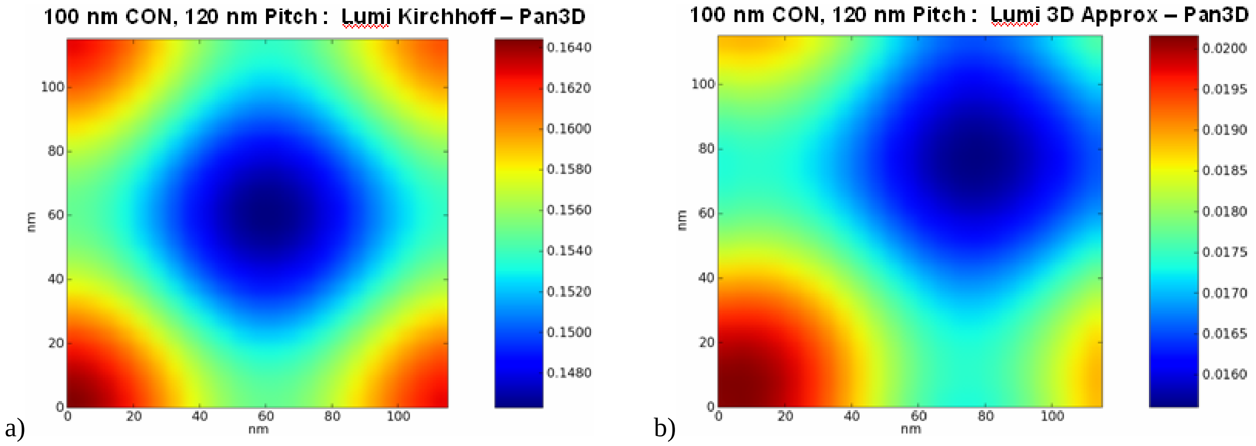

Figure 4. Relative to FDTD, these are aerial image differences of 100 nm contact in 120 nm pitch simulated with a) Luminescent's Kirchhoff and b) 3D approximation. One should note that the scale on b) is a magnitude smaller than a). The 3D approximation is significantly closer to FDTD calculation than Kirchhoff approximation.

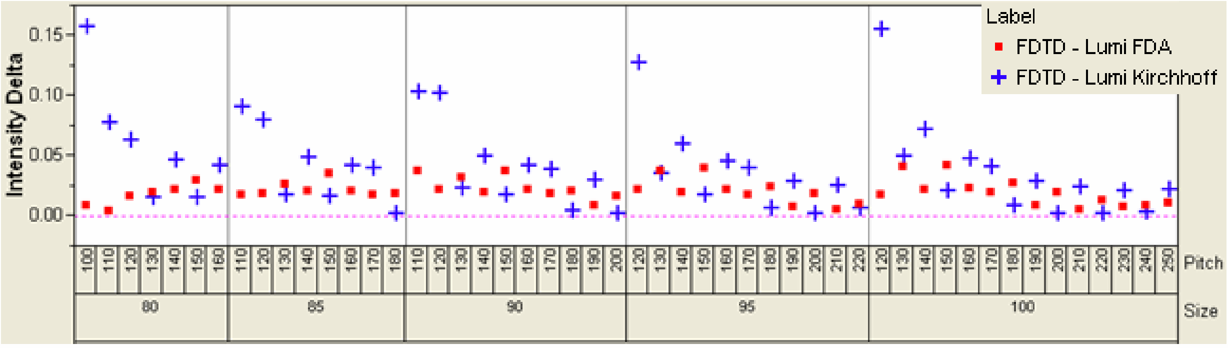

Figure 5. Graph shows the intensity error differences for contact patterns between Luminescent's Kirchhoff and 3D approximation relative to FDTD.

3.2 Results and Discussions for Inversion with FDA

In one of the tests, inversion of an isolated square (100x100nm) with Kirchhoff and a calibrated FDA model resulted in two slightly different mask patterns (Figure 6). The differences between the two patterns included the placements of the SRAFs, the size of the SRAFs, and size of the main feature. The sizes for the Kirchhoff ILT main pattern and SRAF's are generally smaller than the FDA ILT pattern, and this is most likely due to Kirchhoff approximation over predicting the true image intensity. So the inversion process with a Kirchhoff model calculated for a solution with smaller features, while a solution with FDA resulted in larger features. Luminescent estimated the DOF for the Kirchhoff ILT and the FDA patterns were ~200 nm. Both nominal images targeted with less than 0.1 nm EPE at centered cut lines.

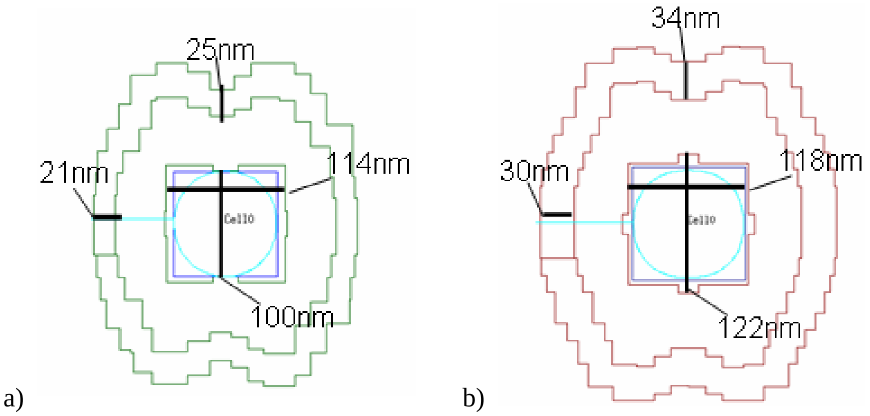

Figure 6. a) ILT solution from Kirchhoff model. b) ILT solution from FDA model.

The two different ILT solutions were simulated in Panoramic with Kirchhoff and FDTD. The matrix of aerial images (Table 1) showed that FDTD simulation of the Kirchhoff ILT pattern had the lowest contrast. This shows a potential consequence of not lithographically accounting for mask 3D effects. A horizontal cut line for the FDTD images showed main feature and SRAF intensity for the Kirchhoff ILT solution was lower than that of the FDA ILT solution by ~19% and ~40%, respectively (Figure 7).

	Kirchhoff ILT	**FDA ILT**
Kirchhoff Simulation	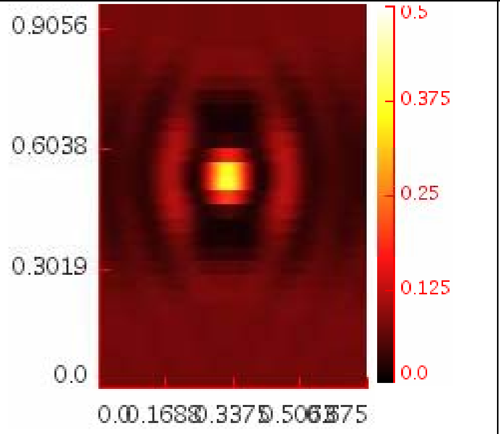	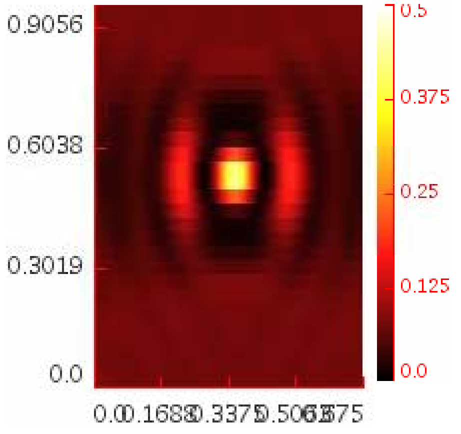
FDTD Simulation	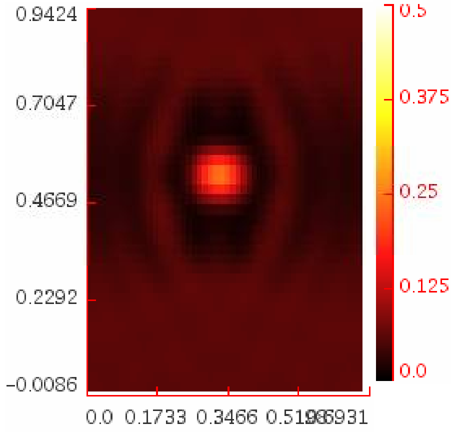	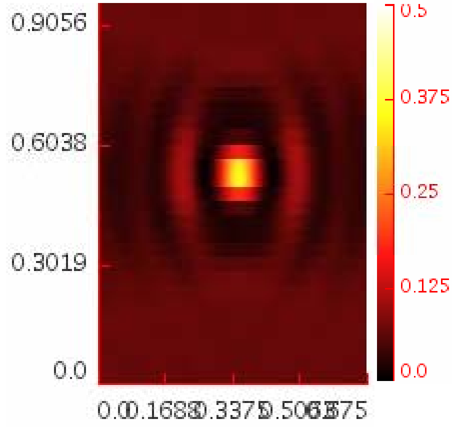

Table 1. Panoramic simulations isolated square ILT solutions from Kirchhoff model and FDA calibrated model.

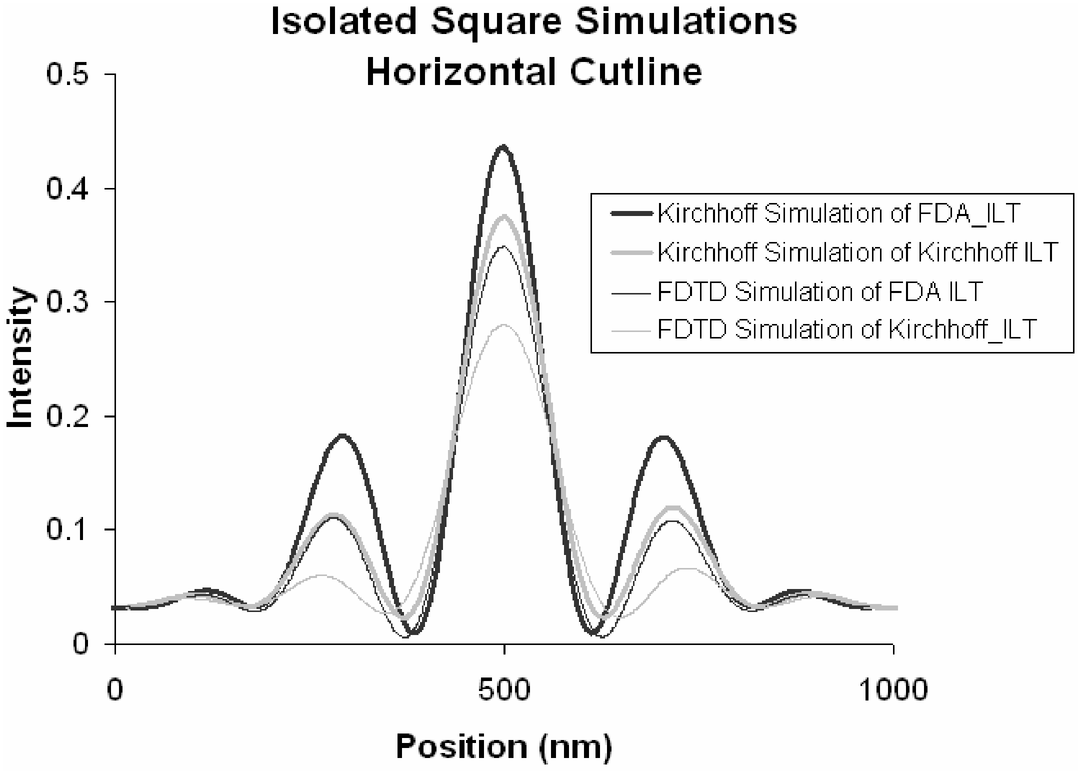

Figure 7. For isolated 100 nm square, FDTD simulation of Kirchhoff and FDA ILT patterns showed FDA ILT image had slightly higher intensity than Kirchhoff ILT image.

Another inversion comparison was conducted with a 1xN array of rectangles (80x400 nm w/350 nm pitch). In general the differences were similar to the isolated square case in that the FDA ILT pattern displayed larger main feature and SRAFs relative to the Kirchhoff ILT pattern (Figure 8). The Kirchhoff ILT pattern had narrowed horizontal center on main feature and perforated SRAFs, while FDA ILT pattern had extended vertical size.

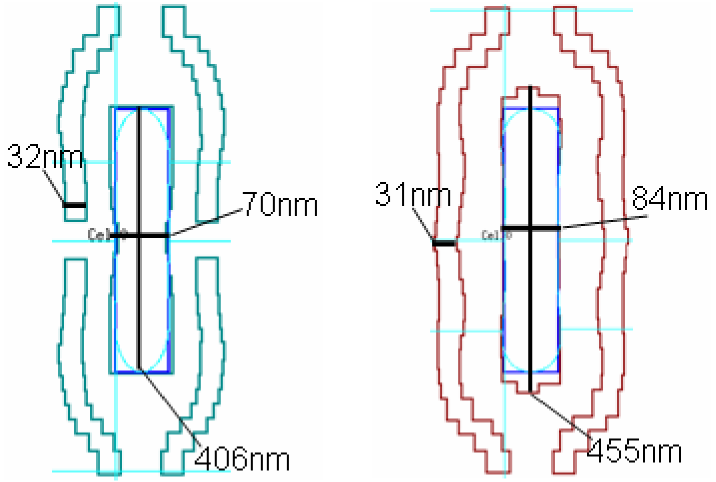

a) b)

Figure 8. ILT generated pattern solutions for nested rectangles with a) Kirchhoff model and b) FDA model.

The two different ILT solutions were also simulated in Panoramic with Kirchhoff and FDTD. The matrix of aerial images (Table 2) showed FDTD aerial images of the Kirchhoff ILT had the lowest contrast, while the Kirchhoff simulation of the FDA ILT had the highest intensity. A horizontal cut line for the FDTD images showed main feature and SRAF intensity for the Kirchhoff ILT solution was lower than that of the FDA ILT solution by ~9% and ~17%, respectively (Figure 9).

	Kirchhoff ILT	**FDA ILT**
Kirchhoff Simulation	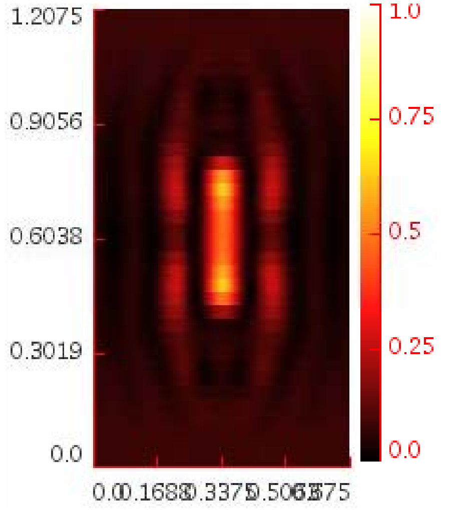	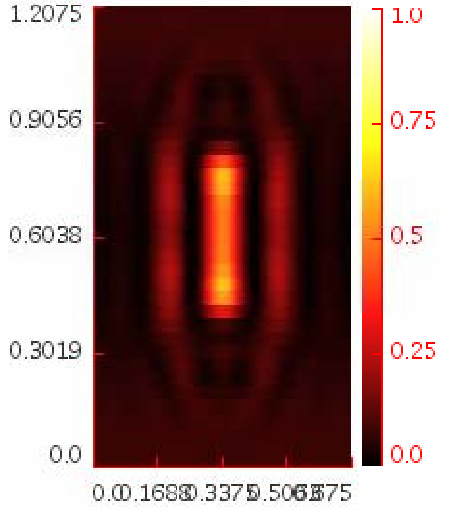
FDTD Simulation	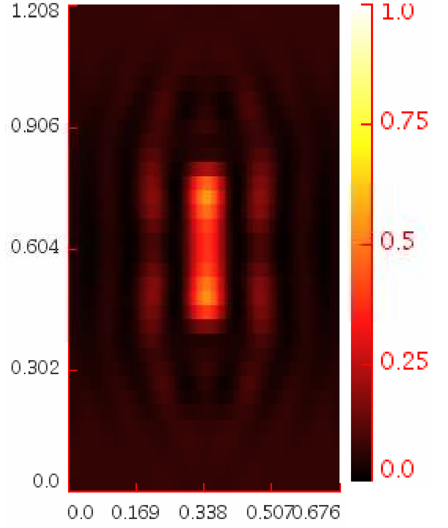	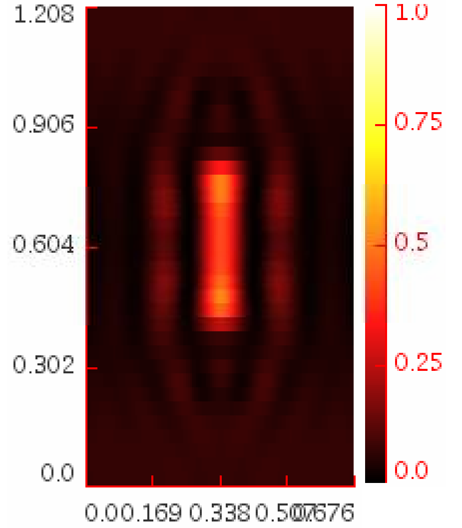

Table 2. Panoramic simulations nested rectangle ILT solutions from Kirchhoff model and FDA calibrated model.

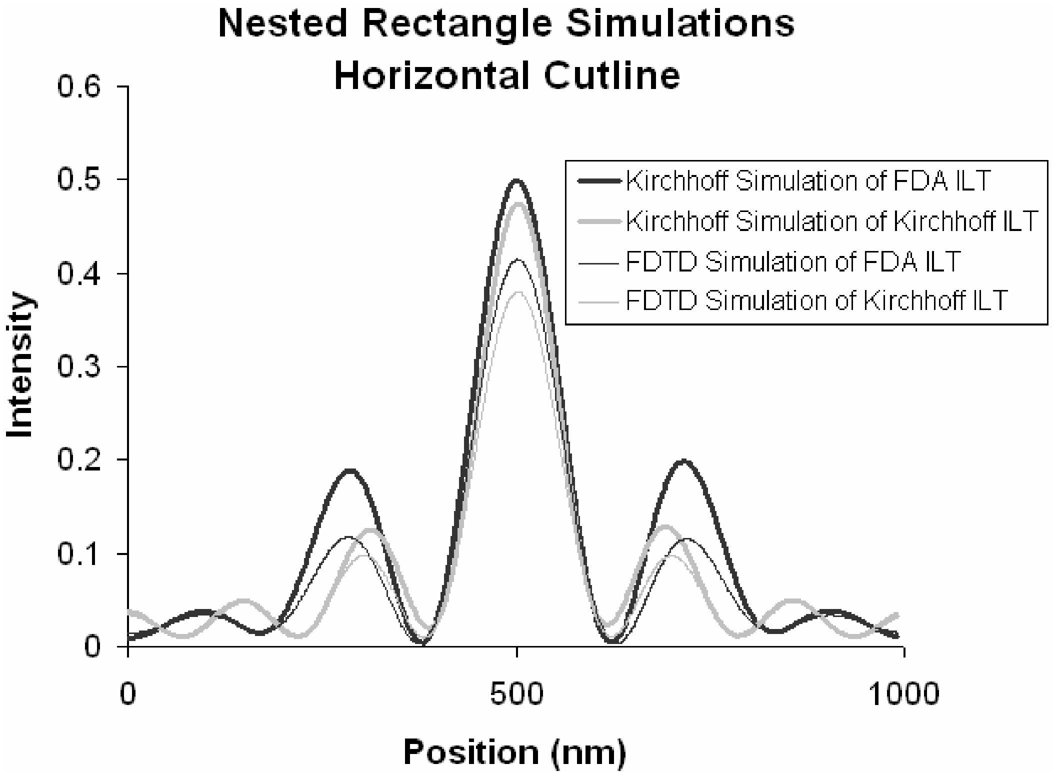

Figure 9. For nested 80 nm rectangles, FDTD simulation of Kirchhoff and FDA ILT patterns showed FDA ILT image had higher intensity profile than Kirchhoff ILT image.

4. CONCLUSIONS

Luminescent has implemented two 3D mask approximation models. On a set of line/space and contact structures, a calibrated FDA model showed less than 0.03 intensity delta relative to rigorous FDTD calculations. Such a calibrated FDA model was successfully employed during inversion on two different patterns. Relative to Kirchhoff ILT patterns, the resulting larger FDA ILT patterns (main features & SRAFs) appeared to be compensating for image degradation from mask topography under oblique illumination. Future collaboration with customer is needed to validate these simulations data with wafer print.

REFERENCES

[1] Jaione Tirapu-Azpiroz et al, Boundary layer model to account for thick mask effects in photolithography, Proc. of SPIE, Vol. 5040, (2003)

[2] Alan Rosenbluth et al, Fast calculation of images for high numerical aperture lithography, Proc. of SPIE, Vol. 5377, (2004)

[3] Sungsoo Suh et al, Three-dimensional mask effect approximate modeling for sub-50nm node device OPC, Proc. Of SPIE, Vol 6521, (2007)

[4] Thomas V. Pistor, Andrew R. Neureuther, & Robert J. Socha, Modeling oblique incidence effects in photomasks, Proc. Of SPIE, 4000, 228 (2000)